Liquid Alumina: Detailed Atomic Coordination Determined from Neutron Diffraction Data Using Empirical Potential Structure Refinement

C. Landron,[1,2] L. Hennet,[1,2] T. E. Jenkins,[3] G. N. Greaves,[3] J. P. Coutures,[4] and A. K. Soper[5,*]
[1]*Centre de Recherches sur les Matériaux à Haute Température, 45071, Orléans Cedex 2, France*
[2]*LURE, 91405, Orsay Cedex, France*
[3]*Department of Physics, University of Wales, Aberystwyth, SY23 3BZ, United Kingdom*
[4]*Institut de Sciences des Matériaux et Génie des Procédés, Université de Perpignan,*
52 Avenue de Villeneuve, 66860 Perpignan Cedex, France
[5]*ISIS Department, Rutherford Appleton Laboratory, Oxon OX11 0QX, United Kingdom*
(Received 24 October 2000)

The neutron scattering structure factor $S_N(Q)$ for a 40 mg drop of molten alumina (Al_2O_3) held at 2500 K, using a laser-heated aerodynamic levitation furnace, is measured for the first time. A 1700 atom model of liquid alumina is generated from these data using the technique of empirical potential structural refinement. About 62% of the aluminum sites are 4-fold coordinated, matching the mostly triply coordinated oxygen sites, but some 24% of the aluminum sites are 5-fold coordinated. The octahedral aluminum sites found in crystalline α-Al_2O_3 occur only at the 2% level in liquid alumina.

DOI: 10.1103/PhysRevLett.86.4839 PACS numbers: 61.12.Ex, 07.20.Ka, 61.20.Ne

There has recently been much interest in developing laser heated gas levitation techniques to examine the structural properties of high temperature and supercooled liquids in general [1], and liquid alumina in particular [2–5]. This is driven by the search for liquid-liquid phase transitions [6], and for local atomic structural changes which occur as a liquid is supercooled [7]. There is often a considerable density deficit between the crystalline and amorphous states. Typically this is 10–15% [8], but it is larger for ionic systems, reaching around 27% in the case of alumina at its melting point, 2326 K [9]. Many of the materials of interest have melting points in excess of 2000 K which, combined with their generally high reactivity, precludes the use of a container in a conventional furnace [1,10–12]. Levitation therefore presents a real opportunity for synthesis and *in situ* characterization of pure liquids or solids at highly elevated temperatures. Materials have been melted with good reproducibility by using acoustic levitation [12–14], electromagnetic levitation [15,16], electrostatic levitation [17,18], as well as aerodynamic levitation [10,11]. The possibility of using aerodynamic levitation in association with CO_2 laser heating [12] to look at the structure of a melt has been demonstrated in recent investigations of refractory oxides [19], including alumina [4,20], using x rays as the structural probe.

We present here the first structural data on molten alumina obtained using neutron diffraction under contactless conditions. The stronger scattering of neutrons by oxygen compared to aluminum serves to highlight the essential structural features of molten aluminum oxide and so complements the existing x-ray data, where the scattering from aluminum is stronger. By employing the empirical potential structure refinement (EPSR) computer simulation procedure [21,22] we are able to obtain for the first time a structural model for liquid alumina which is entirely consistent with the structure factors obtained by both neutrons and x rays, the physical density, and the findings from NMR.

The neutron experiments were carried out on the SANDALS diffractometer at the ISIS spallation neutron source (U.K.). The starting material was a high-purity (99.9%) powder of alumina pressed under isostatic pressure to 250 MPa. The spherical specimens, with a nominal diameter 2.7 mm, corresponding to a weight of 40 mg, were processed by melting them in a CO_2 laser beam and then cooling to room temperature. This size of sample presents a major challenge for a neutron diffraction experiment since the amount of material that can be supported by the levitator is around 1/20th to 1/100th of the amount of material used in a conventional experiment on a liquid. The main change, compared to [10], is the use of horizontal incidence, after a double focusing reflection, of the laser beam onto the sample. As the sphere rotates about a vertical axis, the temperature of the sample is stable and uniform, and the material fully molten: any crystallinity in the sample is readily detectable as sharp Bragg peaks in the diffraction pattern. The argon gas flow used to levitate the sample was precisely adjusted versus temperature by a remote control computer in order to optimize the stability of the sample [23]. The infrared radiation emitted by a 125W CO_2 laser was focused onto the sample by means of spherical mirrors. Our heating system was capable of achieving temperatures well above the melting temperature of alumina $T_m = 2327$ K under both oxidizing and reducing conditions [24], for continuous periods of 20 min. Temperature measurement was performed by means of a calibrated pyrometer.

Figure 1 shows the diffraction pattern from molten aluminum oxide obtained in this experiment, after subtracting the scattering from the boron nitride levitator nozzle. Only neutron detectors above the scattering plane of the nozzle were used to accumulate data, since for detectors below

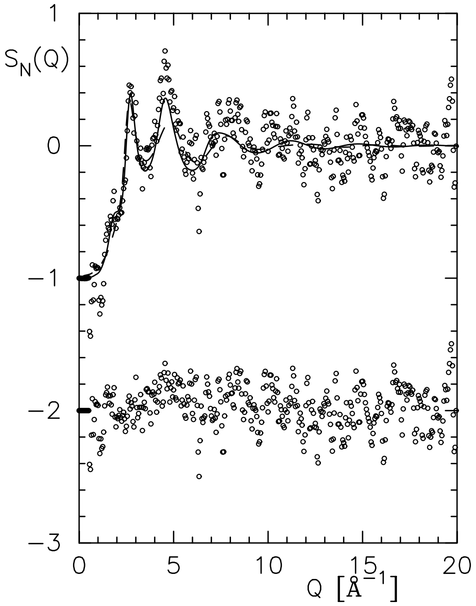

FIG. 1. Experimental neutron structure factor (circles, top) for a 2.7 mm liquid drop of alumina at 2500 K. The dashed line shows the structure factor derived from the model interaction potential described in the text, while the solid line is the fit to the data after empirical potential structure refinement (EPSR). The residual (data minus the fit) is shown at the bottom (circles) and reveals that the structural model derived from EPSR is a good representation of the structure of this liquid.

this plane the scattered neutrons were absorbed in the boron nitride. The data were corrected using the standard ATLAS data analysis package [25], but due to the smallness of the sample could not be put on an absolute scattering cross-section scale. Instead the absolute calibration was determined by choosing the best normalizing factor to give the correct limiting behavior of $S(Q)$ in the limit of large Q. The data shown were aggregated from 5 separate scans on molten alumina, each one occupying about 20 min of neutron beam time.

The neutron structure factor shown in Fig. 1 is in fact a weighted sum of Al-Al, Al-O, and O-O partial structure factors (PSFs): $S_N(Q) = 0.081 S_{\mathrm{AlAl}}(Q) + 0.406 S_{\mathrm{AlO}}(Q) + 0.513 S_{\mathrm{OO}}(Q)$, where the weight factors are independent of Q. This structure factor is dominated by the important AlO and OO terms, whereas the corresponding x-ray diffraction pattern, $S_X(Q)$, is dominated by the AlAl partial structure factor, due to the relatively strong persistence of the Al electron form factor at large Q [26].

Detailed interpretation of these data have been made with EPSR analysis [21,22]. The purpose of this process is to set up realistic ensembles of Al and O ions whose calculated structure factors reproduce the measured structure factors as closely as possible. The simulation was run with 680 Al ions and 1020 O ions in a box of dimension 27.3658 Å give the expected liquid atomic number density (2.81 ± 0.03 g/cm^3 [9]). The starting potential for the simulation was a Lennard-Jones 12-6 potential ($\epsilon_{\mathrm{Al}} = 0.132$ kJ/mole, $\sigma_{\mathrm{Al}} = 1.33$ Å; $\epsilon_{\mathrm{O}} = 0.132$ kJ/mole, $\sigma_{\mathrm{O}} = 3.50$ Å), plus effective charges of $+0.9e$ and $-0.6e$ on the respective ions [27]. The potential was truncated smoothly at half the box dimension and there was no correction for longer range electrostatic interactions. The dashed line in Fig. 1 shows the structure factor obtained with this potential on its own. Subsequent refinements of the liquid structure were achieved by using the difference between simulated and measured structure factors to calculate successive perturbations to the starting potential, until the best possible fit was obtained. In spite of the statistical nature of the data it was found that the quality of fit was quite sensitive to changes in the interatomic potential. The solid line in Fig 1 shows the best fit obtained for these data using this procedure.

A number of molecular dynamics studies of liquid alumina have recently been made [5,26,28,29], including a simulation of the γ-$\mathrm{Al_2O_3}$ radial distribution function (rdf), which bears some similarity with the supercooled state [30]. In all cases the densities employed were higher than the density used here, which was measured directly [9]. Thus, while there are broad similarities between the rdf's of these simulations there are also significant differences [1]. The refinement process described above for the present neutron data produced the set of site-site radial distribution functions (rdfs) shown in Fig. 2. The first peak in the AlO rdf occurs at (1.78 ± 0.05) Å. The uncertainty in this value stems from the low statistical quality of the present data at large Q. The x-ray work [4]

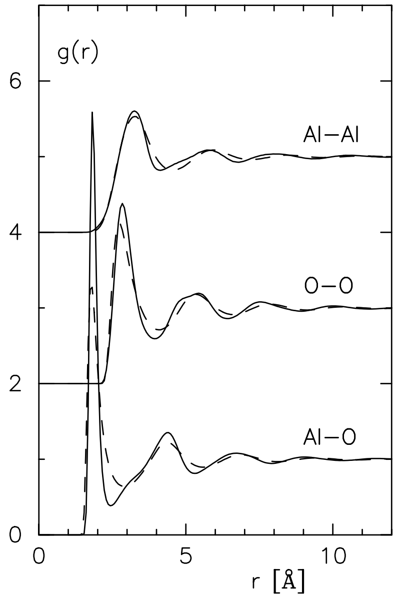

FIG. 2. Site-site radial distribution functions (rdf) for molten alumina, as derived from the model used to fit the data of Fig. 1. The dashed lines show the results of the simulation without structure refinement. We note the strong charge ordering apparent in this liquid, as seen from the oscillations of the AlO rdf being out of phase with those from OO and AlAl.

obtained a value of 1.76 for the first peak, as did an earlier molecular dynamics simulation [5]. It is also notable that the first peak in the OO rdf occurs at a slightly shorter distance, 2.84 Å , compared with the first peak in the AlAl rdf at 3.25 Å. This OO near-neighbor distance is markedly shorter than the 3.08 Å distance derived by Ansell *et al.* [4] from the position of the second peak in their total x-ray rdf. In fact, when appropriately weighted for the x-ray experiment the present partial rdfs combine to give an excellent representation of the previously reported x-ray total rdf for liquid alumina [4]. The second peak in the x-ray rdf is simply a mixture of the shorter OO and longer AlAl distances, giving rise to an average peak position of 3.08 Å.

The coordination number of oxygen about aluminum in our study is 4.2 ± 0.3 atoms, the error embracing the uncertainty in the raw density and fitting the data. This compares well with a value of 4.4 ± 1.0 atoms reported by Ansell *et al.* [4] (even though they assumed the significantly higher density of 3.17 g/cm^3 compared with the present 2.81 g/cm^3), the value of 4.4 obtained by molecular simulation [5], and the value of 4.5 from NMR work [31]. Ansell *et al.* interpreted their data in terms of a transition from octahedral coordination in the solid to tetrahedral coordination of Al in liquid alumina, whereas Waseda *et al.* [3] conclude that the octahedral coordinated aluminum in corundum is retained in the liquid. The NMR data [2] were initially interpreted as indicating that liquid alumina consisted of a mixture of 4-fold and 6-fold coordinated Al sites undergoing rapid exchange, resulting in an average coordination number of 4.5. Poe *et al.* later suggested the presence of 5-fold coordinated Al in liquid alumina [5], the mean coordination number being the average of 4-, 5-, and 6-fold sites [31].

To throw light on these issues, the distributions of coordination numbers for aluminum and oxygen, as revealed by our simulations, are shown in Fig. 3. It is found that there is a distribution of coordination numbers between 3 and 6 oxygen atoms about aluminum, and 2 to 4 aluminums about oxygen. As can be seen in this figure, about 24% of the aluminum atoms are 5-fold coordinated, with some octahedral coordinations as well, so the aluminum coordination is not purely 4-fold. We have investigated the geometry of the AlO_4 and AlO_5 coordination units in our model, and find that, while the 4-fold sites are mostly tetrahedral, the 5-fold sites are often octahedral in arrangement with an oxygen vacancy (Fig. 4). Further analysis of the local coordination environment in the simulation finds little preference for 6-fold coordinated Al to be surrounded by other 6-fold Al, so there is no indication at this stage whether this liquid is a likely candidate for a liquid-liquid phase transition. We have refitted the neutron scattering data to different densities and find that the different coordination units remain the same, the principal change being their relative populations. For this reason we have considerable confidence in the local coordinations revealed here.

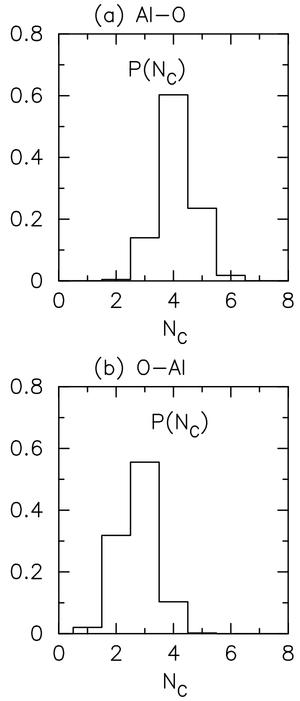

FIG. 3. Probability distribution of coordination numbers (a) O about Al, and (b) Al about O. We note the presence of about 25% 5-fold coordinated, and some 6-fold coordinated, aluminum atoms.

In summary, it is now clear that an important clue to the marked change in density which occurs when alumina melts lies in the transition from octahedral coordination of the aluminum in the solid state to predominantly tetrahedral coordination in the liquid, although remnants of the crystalline octahedral coordination are still present at the 24% level. The reduced coordination numbers of O about Al, and Al about O, which we have deduced from the neutron scattering data, reflect the lower density of this high temperature liquid compared with α-Al_2O_3, but we envisage that the local arrangements of aluminum and oxygen atoms are constantly switching through the minor

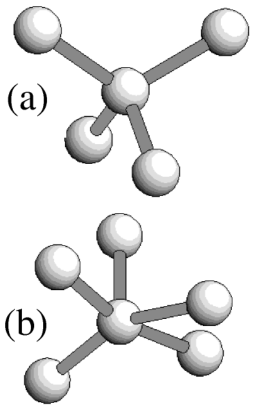

FIG. 4. Typical 4-fold (a) and 5-fold (b) coordinations of aluminum found in the computer simulation of liquid alumina.

configurations AlO_3, AlO_6, OAl_2, and OAl_4. The significant progress signaled by this work is that it is the first demonstration of levitation furnace experiments with neutrons, and this is successfully combined with a technique for building an atomic model of the liquid which is consistent with both the present neutron data, and the earlier x-ray and NMR data.

This work was financially supported by the CNRS and a contract "XIème contrat de plan Etat/Région." The authors are grateful to D. Ruffier and Y. Auger for the construction of the analysis cell, and for the considerable efforts made by the ISIS support staff.

---

*Corresponding author.
Also at Department of Physics and Astronomy, University College London, Gower Street, London WC1E 6BT, U.K.

[1] S. Krishnan and D. L. Price, J. Phys. Condens. Matter **12**, R145 (2000).

[2] J. P. Coutures, D. Massiott, C. Bessada, P. Echegat, J-C. Rifflet, and F. Traulelle, C.R. Acad. Sci. **310**, 1041 (1990).

[3] Y. Waseda, K. Sugiyama, and J. M. Toguri, Z. Naturforsch. A **50**, 770 (1995).

[4] S. Ansell, S. Krishnan, J. K. Weber, J. J. Felten, P. C. Nordine, M. A. Beno, D. L. Price, and M.-L. Saboungi, Phys. Rev. Lett. **78**, 464 (1997).

[5] B. T. Poe, P. F. McMillan, B. Cote, D. Masiiot, and J-P. Coutures, J. Phys. Chem. **96**, 8220 (1992).

[6] S. Aasland and P. F. McMillan, Nature (London) **369**, 633 (1994).

[7] D. Massiot, D. Trumeau, B. Touzo, I. Farnam, J-C. Rifflet, A. Douy, and J-P. Coutures, J. Phys. Chem. **99**, 16 455 (1995).

[8] J. Zarzycki, in *Glasses and the Vitreous State* (Cambridge University Press, Cambridge, England, 1991), p. 11.

[9] B. Glorieux, F. Millot, J. C. Rifflet, and J-P. Coutures, Int. J. Thermophys. **20**, 1085–1094 (1999). This work demonstrates the differences between density measurements made using crucibles and contactless furnaces. The values obtained in the latter case are significantly lower for liquid alumina than those quoted previously: P. Tyrolerova and W. K. Lu, J. Am. Ceram. Soc. **52**, 77 (1969).

[10] C. Landron, L. Hennet, J. P. Coutures, T. Jenkins, C. Alétru, G. N. Greaves, A. K. Soper, and G. Derbyshire, Rev. Sci. Instrum. **71**, 1745 (2000).

[11] S. Krishnan, S. Ansell, and D. L. Price, J. Non-Cryst. Solids **250**, 286 (1999).

[12] W. A. Oran and L. H. Berge, Rev. Sci. Instrum. **53**, 851 (1982).

[13] E. H. Trinh and C. J. Hsu, J. Acoust. Soc. Am. **6**, 1757 (1986).

[14] P. C. Nordine, Ceram. Bull. **70**, 71 (1991).

[15] S. Krishnan, G. P. Hansen, R. H. Hauge, and G. P. Margrave, Metall. Trans. A **19**, 1939 (1988).

[16] G. Jacobs and I. Egry, Phys. Rev. **59**, 3961 (1999).

[17] T. F. Clancy, E. G. Lierke, R. Grossbach, and W. M. Heide, Acta Astronaut. **7**, 877 (1980).

[18] W. K. Rhim, K. Osahka, J. F. Paradis, and R. E. Spjut, Rev. Sci. Instrum. **70**, 2796 (1999).

[19] S. Krishnan, S. Ansell, and D. L. Price, J. Am. Ceram. Soc. **81**, 1967 (1998).

[20] J. K. Weber, S. Krishnan, C. D. Anderson, and P. C. Nordine, J. Am. Ceram. Soc. **78**, 583 (1995).

[21] A. K. Soper, Chem. Phys. **202**, 295 (1996).

[22] A. K. Soper, Chem. Phys. **258**, 121 (2000).

[23] C. Landron, X. Launay, J. C. Rifflet, Y. Auger, D. Ruffier, J. P. Coutures, M. Lemonier, M. Gailhanou, M. Bessière, D. Bazin, and H. Dexpert, Nucl. Instrum. Methods Phys. Res., Sect. B **124**, 627 (1997).

[24] C. Landron, L. Hennet, J. P. Coutures, M. Gailhanou, M. Gramond, and J. F. Berar, Europhys. Lett. **44**, 429 (1998).

[25] A. K. Soper, W. S. Howells, and A. C. Hannon, Rutherford Appleton Laboratory Report No. RAL-89-046, 1989.

[26] M. Hemmati, M. Wilson, and P. A. Madden, J. Phys. Chem. B **103**, 4023 (1999).

[27] An exhaustive search of parameter space for this potential was not made. The charges were chosen to be as large as possible while avoiding crystallization in the simulated ensemble at the working temperature of the experiment. The σ values were chosen to give the best possible reproduction of the neutron data without empirical potential refinement (dashed line in Fig. 1). These values have an uncertainty of $\sim\pm 0.02$ Å.

[28] M. A. San Miguel, J. F. Sanz, L. J. Alvarez, and J. A. Odriozola, Phys. Rev. B **58**, 2369 (1998).

[29] G. Gutiérrez, A. B. Belonoshko, R. Ahuja, and B. Johansson, Phys. Rev. E (to be published).

[30] L. J. Álvarez, L. E. Léon, J. F. Sanz, M. J. Capitán, and J. A. Odriozola, J. Phys. Chem. **99**, 17 872 (1995).

[31] P. Florian, D. Massiot, B. Poe, I. Farman, and J-P. Coutures, Solid State Magn. Reson. **5**, 233 (1995).